

## Activation of Caspase-3 in Developmental Models of Programmed Cell Death in Neurons of the Substantia Nigra

\*Beom S. Jeon, \*Nikolai G. Kholodilov, \*Tinmarla F. Oo, \*Sang-Yun Kim,  
†Kevin J. Tomaselli, †Anu Srinivasan, \*‡Leonidas Stefanis, and \*‡Robert E. Burke

Departments of \*Neurology and ‡Pathology, Columbia University College of Physicians and Surgeons, New York, New York;  
and †IDUN Pharmaceuticals, La Jolla, California, U.S.A.

**Abstract:** Programmed cell death has been proposed to play a role in the death of neurons in acute and chronic degenerative neurologic disease. There is now evidence that the caspases, a family of cysteine proteases, mediate programmed cell death in various cells. In neurons, caspase-3 (CPP32/Yama/apopain), in particular, has been proposed to play a role. We examined the expression of caspase-3 in three models of programmed cell death affecting neurons of the substantia nigra in the rat: natural developmental neuron death and induced developmental death following either striatal target injury with quinolinic acid or dopamine terminal lesion with intrastriatal injection of 6-hydroxydopamine. Using an antibody to the large (p17) subunit of activated caspase-3, we have found that activated enzyme is expressed in apoptotic profiles in all models. Increased p17 immunostaining correlated with increased enzyme activity. The subcellular distribution of activated caspase-3 differed among the models: In natural cell death and the target injury model, it was strictly nuclear, whereas in the toxin model, it was also cytoplasmic. We conclude that p17 immunostaining is a useful marker for programmed cell death in neurons of the substantia nigra. **Key Words:** Programmed cell death—Apoptosis—Caspase—Substantia nigra—Parkinson's disease. *J. Neurochem.* **73**, 322–333 (1999).

During the normal development of the CNS, substantial numbers of neurons die due to programmed cell death (PCD) (Cowan et al., 1984; Clarke, 1985; Oppenheim, 1991; Hamburger, 1992). In many, but not all, instances of PCD during development, the dying neurons demonstrate a characteristic morphologic appearance, termed apoptosis (Kerr et al., 1972). There is considerable evidence that PCD is mediated by genetic programs intrinsic to the cell (Ellis et al., 1991; Johnson and Deckwerth, 1993; Jacobson et al., 1997). There is growing evidence that PCD may also play a role in pathologic neuron deaths in the CNS, in acute brain injuries such as stroke and trauma, and in chronic degenerative neurologic diseases such as Alzheimer's disease and Parkinson's disease (PD) (Bredesen, 1995; Thompson, 1995;

Stefanis et al., 1997). The important implication of this concept is that pharmacologic or genetic blockade of the molecular pathways of PCD may prevent neuronal death in these settings, leading to new forms of therapeutic intervention.

Many important new insights into the molecular mechanisms of PCD have derived from studies of developmental cell death in the nematode *Caenorhabditis elegans* (Ellis et al., 1991). One of the genes necessary for cell death in this organism is *ced-3* (Ellis et al., 1991), which has been shown to be homologous to mammalian interleukin-1 $\beta$  converting enzyme, a cysteine protease (Yuan et al., 1993). Other aspartate-specific cysteine proteases (caspases) have been subsequently identified (Alnemri et al., 1996; Alnemri, 1997). Evidence implicating these proteases in PCD includes observations that their ectopic expression in cell lines induces apoptotic death (Miura et al., 1993) and that their inhibition, by either viral proteins, such as CrmA (Enari et al., 1995; Tewari et al., 1995), or specific peptide inhibitors based on the cleavage site, such as YVAD (Enari et al., 1995; Milligan et al., 1995), inhibits apoptotic death. All of the caspases are synthesized in a proenzyme form, which is cleaved at an aspartate to yield a larger (p17–p20) and a smaller subunit (p10–p12), which heterodimerize to form an enzymatically active form.

Among the caspases, caspase-3 (CPP32/Yama/apopain) (Fernandes-Alnemri et al., 1994; Nicholson et al., 1995; Tewari et al., 1995) is of particular interest in

---

Received January 18, 1999; revised manuscript received February 25, 1999; accepted February 26, 1999.

Address correspondence and reprint requests to Dr. R. E. Burke at Department of Neurology, Box 67, Columbia University College of Physicians and Surgeons, 710 West 168th Street, New York, NY 10032, U.S.A.

*Abbreviations used:* BSA, bovine serum albumin; 6-OHDA, 6-hydroxydopamine; PBS, phosphate-buffered saline; PCD, programmed cell death; PD, Parkinson's disease; PND, postnatal day; RPA, ribonuclease protection assay; SDS, sodium dodecyl sulfate; SN, substantia nigra; SNpc, substantia nigra pars compacta; SSC, saline–sodium citrate; TUNEL, terminal deoxynucleotidyltransferase-mediated dUTP nick end-labeling.

relation to neuronal death. It has been shown to be activated *in vitro* on induction of PCD in postnatal cerebellar granule neurons (Armstrong et al., 1997; Du et al., 1997) and embryonic mouse neurons (Keane et al., 1997). Strong evidence for a role for caspase-3 in mediating developmental neuronal death derives from observations made in knockout mice, which demonstrate hyperplastic brains due to supernumerary cells (Kuida et al., 1996). There is also evidence of caspase-3 activation *in vivo* in models of induced retinal ganglion cell death following axotomy (Kermer et al., 1998) and acute brain injury due to either trauma (Yakovlev et al., 1997) or stroke (Chen et al., 1998; Namura et al., 1998). However, less is known about caspase-3 expression in models of PCD related to chronic degenerative neurologic diseases.

We have had an interest in the molecular basis of PCD in neurons of the substantia nigra (SN). The dopamine neurons of the SN pars compacta (SNpc) are the principal neurons to degenerate in idiopathic PD, and it has been suggested, but not proven, that neuron death in this disorder may be mediated by PCD (Mochizuki et al., 1996; Tompkins et al., 1997). We have shown that natural cell death, with the morphology of apoptosis, occurs in dopamine neurons of the SNpc (Janec and Burke, 1993; Oo and Burke, 1997) and that this death event can be augmented ~10-fold by developmental injury to the target striatum (Macaya et al., 1994). In this striatal target injury model, cell death is demonstrated to be exclusively and definitively apoptotic by suppressed silver staining, ultrastructural analysis, and terminal deoxynucleotidyltransferase-mediated dUTP nick end-labeling (TUNEL) (Macaya et al., 1994). We have proposed that induced death in SNpc in this model is due to the loss of target-derived retrograde support, as envisioned by classic neurotrophic theory (Barde, 1989). This hypothesis is supported by the observation that developmental destruction of intrastriatal dopamine terminals with the selective neurotoxin 6-hydroxydopamine (6-OHDA), resulting in disruption of target interaction at the terminal level, also results in the induction of apoptosis in dopamine neurons of the SNpc (Marti et al., 1997). The 6-OHDA model is of particular interest in relation to the pathogenesis of degenerative disease, because apoptotic death was induced even after the developmental period and because 6-OHDA is widely used to create animal models of parkinsonism (Ungerstedt, 1971; Sauer and Oertel, 1994).

In this study we sought to address whether activation of caspase-3 plays a role in PCD in neurons of the SN and, if it does, whether its activation is a general feature of PCD in these models. In addition, there has been relatively little information available about the cellular localization of activated caspase-3 in neurons that undergo PCD in living animal models. In this study we examined at the cellular level the localization of activated caspase-3 by performing immunohistochemistry with an antiserum that specifically recognizes the p17 subunit of activated caspase-3 (Armstrong et al., 1997; Namura et al., 1998). We sought to determine whether

similar or distinctive patterns of cellular localization are observed in these models. Finally, we sought also to determine, if caspase-3 is activated, whether its activation is mediated at a transcriptional level, as observed in some studies (Chen et al., 1998), or posttranscriptionally, as observed in others (Du et al., 1997).

## MATERIALS AND METHODS

### Striatal lesions with quinolinic acid

Striatal quinolinic acid lesions were performed as previously described (Macaya et al., 1994; Kelly and Burke, 1996) on postnatal day (PND) 7 or 12 rats: Following induction of methoxyflurane (Metofane; Pittman-Moore) anesthesia, a 28-gauge cannula was inserted into the striatum at 3.0 mm left of and 0.5 mm anterior to bregma, at a depth of 4.0 mm. Quinolinic acid (480 nmol/ $\mu$ l) in 0.1 M phosphate-buffered saline (PBS; pH 7.4) was infused by pump at 1.0  $\mu$ l/2.0 min. PND 12 animals were used only in the immunohistochemical studies, to facilitate tissue processing. We have previously shown that the magnitude, distribution, and morphology of cell death in SN are identical between PND 7 and PND 14 (Kelly and Burke, 1996). This protocol has been approved by the Animal Care and Use Committee at Columbia-Presbyterian Medical Center.

### 6-OHDA lesions

6-OHDA lesions were performed as previously described (Marti et al., 1997). Pups were pretreated with 25 mg/kg desmethylimipramine, anesthetized by inhalation of Metofane, and placed prone on an ice pack. The skull was exposed by a midline incision, and a burr hole was placed 3.0 mm lateral to the left of bregma on the coronal suture. A 28-gauge cannula was then inserted vertically into the striatum to a depth of 4.0 mm from the top of the skull. 6-OHDA hydrobromide (Regis) was prepared at 15  $\mu$ g (total weight)/1.0  $\mu$ l in 0.9% NaCl containing 0.02% ascorbic acid and infused by pump (CMA/100; Carnegie Medicin) at a rate of 0.25  $\mu$ l/min. The cannula was slowly withdrawn 2 min after the end of the infusion. After recovery from anesthesia, pups were returned to the dams until the assigned postlesion day.

### Histology

PND 12 rat pups were anesthetized with Metofane, a thoracotomy was performed, and the left cardiac ventricle was cannulated with a 20-gauge needle. Each animal was then perfused with ice-cold 0.9% NaCl by gravity for 5 min. They were then perfused with ice-cold 4% paraformaldehyde in 0.1 M phosphate buffer by gravity for 10 min. The brain was then carefully removed from the skull, postfixed in the same fixative for 3 h at 4°C, and then cryoprotected in 20% sucrose in 0.1 M phosphate buffer for 24 h. The brains were then rapidly frozen in 2-methylbutane chilled on dry ice and sectioned through the entire SN at 20  $\mu$ m on a cryostat. Sections were collected into PBS and processed free-floating. They were first treated in 0.1 M PBS (pH 7.1) containing 0.5% bovine serum albumin (BSA) and then in PBS containing BSA and 0.1% Triton X-100 at 4°C with shaking for 30 min. After a wash in PBS, sections were incubated for 48 h with a rabbit polyclonal antiserum (CM1), which recognizes the caspase-3 p17 subunit, at 1:1,000 in PBS containing BSA with shaking at 4°C. Sections were washed and then incubated with biotinylated protein A, prepared in this laboratory, at 1:100 in PBS containing BSA for 60 min at room temperature. Following additional washes, sections were incubated with avidin-biotin-horseradish peroxidase complexes

(Vector Labs) at 1:600 for 60 min at room temperature. Following washes in PBS, sections were incubated in a solution of diaminobenzidine (50 mg in 100 ml of Tris buffer, pH 7.6) containing glucose oxidase, ammonium chloride, and D(+)-glucose to generate H<sub>2</sub>O<sub>2</sub>. The antiserum to the p17 subunit was raised against <sup>163</sup>CRGTELDGCIETD<sup>175</sup>, corresponding to the C terminus of the human p17 fragment, and affinity-purified against the peptide. On immunoblots this antiserum recognizes the caspase p17–18 band but not the unprocessed zymogen or the p10 processed band (Armstrong et al., 1997; Namura et al., 1998; Srinivasan et al., 1998).

After immunoperoxidase staining, sections were mounted on subbed glass slides and counterstained with thionin. This procedure made it possible to identify neuronal morphology and discrete, rounded intranuclear chromatin clumps characteristic of apoptosis. We have previously shown in the striatal lesion model that chromatin clumps identified with basophilic dyes are confirmed at the ultrastructural level to be apoptotic (Macaya et al., 1994). Furthermore, in both the striatal lesion and the 6-OHDA models, basophilic apoptotic chromatin clumps can be demonstrated within TUNEL-positive (Gavrieli et al., 1992) profiles (Macaya et al., 1994; Marti et al., 1997). In our experience the TUNEL technique (Wijsman et al., 1993) is less sensitive for apoptotic morphology than thionin staining, presumably owing to limits on tissue penetration by macromolecular reagents.

Apoptotic profiles in each SN were quantified by selecting two sections from each of SN planes 4.2, 3.7, and 3.2 from the atlas of Paxinos and Watson (1982) and scanning the entire SN at ×600. Apoptotic profiles were identified as cellular profiles containing one or more distinct, rounded basophilic chromatin clumps. Free extracellular chromatin clumps, lying outside an identifiable cellular profile, were not counted. The number of profiles in the two sections in a given plane was averaged, to provide a measure for that plane, and then the averages for the three planes were added to provide an index of the number of profiles for each SN. We have previously shown, using a physical dissector technique (Gundersen, 1986), that apoptotic profiles, as defined, are rarely split by the microtome blade (Oo and Burke, 1997). Clarke and Oppenheim (1995) have demonstrated a similar result. Thus apoptotic profiles, identified by focusing through the section, represent unique and unbiased counts.

### Northern analysis

The SN was microdissected at 4 and 24 h after quinolinic acid injection and at 24, 48, and 72 h after 6-OHDA injection. Each brain was placed in a rat brain matrix on ice, and a 2-mm coronal section of the midbrain was taken. The coronal section was placed posterior surface down on an ice-cold glass plate, and the SN was visualized. A horizontal cut was made below the cerebral aqueduct, and the dorsal piece was discarded. The ventral piece was divided midsagittally into the left (experimental) and right (control) SN, which were then frozen on dry ice and stored at –80°C until RNA isolation. RNA was isolated from each SN individually using a Qiagen RNeasy minikit. Each piece of tissue, weighing ~10 mg, was homogenized in 350 μl of buffer provided by passing it through a 22-gauge needle with a 1-ml syringe 10 times. Further steps of the RNA isolation were carried out according to the manufacturer's instructions. RNA concentration was then determined by measuring absorption at 260 nm on a GenQuant spectrophotometer (Pharmacia). Ten micrograms of each RNA sample per lane was electrophoresed in 1.4% agarose-formaldehyde gel and transferred onto a Hybond-N membrane (Amersham) using a

capillary system (Sambrook et al., 1989) overnight in 2× saline–sodium citrate (SSC). After transferring, RNA was cross-linked to the membrane by UV exposure in a FUNA-UV-Linker (Spectrolone).

To create a probe for northern analysis, oligonucleotide primers for the coding region of the rat caspase-3 were designed based on its published sequence (accession no. U34685). Primers were synthesized by GenSet (La Jolla, CA, U.S.A.). The forward primer was 5'-TCATGGCCCTGAAAT-ACG-3', and the reverse primer was 5'-TGAAGAGTTTCG-GCTTTCC-3'. One microgram of the SN RNA was used for cDNA synthesis with a Promega reverse transcription system using the recommended conditions. Two microliters of cDNA was then used for PCR, which was carried out in 20 μl of reaction mixture provided by Promega with *Taq* DNA polymerase. PCR was performed in an Omni-E cycler (Hybaid) as follows: 5 min at 95°C; 35 cycles of 30 s at 94°C, 30 s at 55°C, and 20 s at 72°C; and final elongation for 7 min at 74°C. The 243-bp PCR product was cloned in pGEM-T vector (Promega), and its sequence was confirmed by automated sequencing. Purified plasmid (100–500 ng) was linearized by cutting with *Sa*I and used for generation of a <sup>32</sup>P-labeled antisense riboprobe with a transcription system and T7 RNA polymerase from Promega.

Hybridization was performed overnight at 67°C in a mixture containing 5× SSC, 5× Denhardt's solution, and 0.2% sodium dodecyl sulfate (SDS). Washing was carried out three times in a solution containing 0.2× SSC and 0.2% SDS at 65°C. The membrane was then dried in air, wrapped, and exposed to Biomax x-ray film (Kodak).

### Ribonuclease protection assay (RPA)

RPA was performed using a Hybspeed RPA kit (Ambion). Five micrograms of total RNA from each SN, microdissected as described above, was aliquoted into a 0.5-ml thin-walled microcentrifuge tube (Marsh, U.S.A.). From 0.25 to 5 pg of caspase-3 sense RNA, synthesized using the cDNA clone described above and a Promega transcription system, served as standards in five lanes of each gel. RNA was mixed with labeled caspase-3 antisense riboprobe (500,000 cpm per lane; prepared as described above) and 0.5 μg of yeast RNA and then coprecipitated with 0.1 volume of 3.0 M of NH<sub>4</sub>Cl, 2 volumes of 100% ethanol, and 2 μl of Pellet-Point (Novagen). The pellet was washed with 200 μl of 70% ethanol and then with 100 μl of 100% ethanol. The pellet was air-dried for 5 min and then dissolved in 10 μl of hybridization buffer preheated to 95°C. The mixture was denatured at 95°C for 3 min, and then hybridization was performed in 68°C for 20 min. Nonhybridized RNA was digested with 100 μl of diluted RNase A/T1 mix at 1:100 in RNase digestion buffer at 37°C for 30 min. Hybspeed Inactivation/Precipitation Mix (150 μl) was added, and the mixture was placed at –20°C overnight. The mixture was centrifuged for 15 min, and the supernatant was carefully discarded. The pellet was dissolved in 15 μl of loading buffer, loaded onto 6% polyacrylamide nondenaturing gel, and electrophoresed at 140 V for 3 h. After electrophoresis, the gel was dried in a gel dryer (Bio-Rad) and exposed to Kodak Biomax x-ray film. The optical density of the protected band was measured, and the amount of caspase-3 mRNA was determined from a standard curve based on the optical densities of the synthetic caspase-3 standards.

### In situ hybridization

For in situ hybridization, rats were killed at 4 or 24 h after striatal lesion. Rats were perfused intracardially with chilled

saline for 5 min, and the brains were then rapidly removed and frozen by immersion in 2-methylbutane on dry ice. The brains were then serially sectioned through the SN at 15  $\mu\text{m}$ . Sections were thaw-mounted onto subbed slides and stored at  $-80^{\circ}\text{C}$  until use. For hybridization, sections were warmed to room temperature and then fixed by immersion in 4% paraformaldehyde in 0.1 M phosphate buffer (pH 7.1) for 7 min, rinsed twice in PBS, and delipidated by successive immersion in higher concentrations of ethanol and then chloroform. Sections were prehybridized at  $40^{\circ}\text{C}$  for 2 h with formamide/prehybridization mix (1:1 vol/vol) as previously described (Burke et al., 1994). Sections were then hybridized with formamide/hybridization mix (1:1 vol/vol) at  $40^{\circ}\text{C}$  overnight. Labeled riboprobe (prepared as described above) was added to a final activity of  $\sim 6,000$  cpm/ $\mu\text{l}$  of the 1:1 (vol/vol) formamide/hybridization solution. Following hybridizations, sections were washed in  $2\times$  SSC and then treated with RNase at  $37^{\circ}\text{C}$  for 30 min. They were then washed in  $2\times$  SSC for 60 min at  $50^{\circ}\text{C}$ , followed by immersion in 4 L of  $0.1\times$  SSC containing 0.05% sodium pyrophosphate and 14 mM  $\beta$ -mercaptoethanol at  $40^{\circ}\text{C}$  for 3 h with gentle stirring. Sections remained in this wash at room temperature overnight. They were then dehydrated in ethanol, vacuum-dried, and apposed to x-ray film at  $-80^{\circ}\text{C}$  for 3–4 weeks.  $^{14}\text{C}$  standards embedded in plastic (Amersham) were enclosed in each cassette. Relative optical density measurements for the SNpc were made with a Loats Associates Inquiry image analysis system, as previously described (Burke et al., 1994).

### Western analysis

Individual pieces of SN were homogenized as described above, using a 1-ml syringe and 22-gauge needle, with homogenizing buffer (100  $\mu\text{l}$  per piece) containing 10 mM Tris-HCl (pH 7.5), 2 mM EDTA, 0.5 mM EGTA, 20  $\mu\text{g}/\text{ml}$  leupeptin hemisulfate, and 17  $\mu\text{g}/\text{ml}$  phenylmethylsulfonyl fluoride (Boehringer). The homogenate was boiled for 5 min, 10  $\mu\text{l}$  of 10% SDS was then added, and the mixture was kept on ice for 1 h. It was boiled again for 3 min and centrifuged for 10 min at 14,000 g at  $4^{\circ}\text{C}$ . The supernatant was collected. The protein concentration of the supernatant was measured using a micro BCA kit (Pierce) and UV spectrophotometer at 562 nm (UV 160; Shimadzu Scientific Instruments). The sample buffer (Novex) was added to the supernatant to bring the protein concentration to 5  $\mu\text{g}/\mu\text{l}$ , and then  $\beta$ -mercaptoethanol was added to 4%. The mixtures were boiled for 1 min, and 10  $\mu\text{l}$  of the mixture containing 50  $\mu\text{g}$  of protein was electrophoresed on a 15% SDS-polyacrylamide gel for 3 h at 300 V. After electrophoresis, proteins were transferred to a PVDF (polyvinylidene difluoride) membrane (Amersham) using a semidry electroblotter (E&K Scientific Products). The membrane was blocked overnight in 0.1 M PBS (pH 7.5) containing 0.1% Tween 20 and 5% dry milk at  $4^{\circ}\text{C}$ . The membrane was probed with primary antibody [anti-human apopain/CPP32 p12 subunit (Upstate Biotechnology) at 1:1,000 or anti-p17 (CM1) at 1:2,000] in blocking solution for 48 h at  $4^{\circ}\text{C}$  and then washed three times for 15 min each with blocking solution. The membrane was incubated with secondary antibody conjugated with horseradish peroxidase (anti-rabbit IgG; Amersham), diluted at 1:2,500 in the blocking solution for 1 h at room temperature. The membrane was washed in PBS-Tween six times for 20 min each. Protein bands were detected by a chemiluminescent technique (Supersignal Ultra Substrate; Pierce) and exposure to Biomax x-ray film (Kodak).

### Fluorometric assay of caspase-3 activity

To serve as a positive control for caspase-3 activity, PC12 cells were grown as described previously (Stefanis et al., 1996), and then serum was withdrawn for 3 h. At that time, cells were rinsed in cold PBS and collected in a buffer of 25 mM HEPES (pH 7.5), 5 mM EDTA, 1 mM EGTA, 5 mM  $\text{MgCl}_2$ , 5 mM dithiothreitol, 10  $\mu\text{g}/\text{ml}$  each pepstatin and leupeptin, and 1 mM phenylmethylsulfonyl fluoride. The cellular material was left for 20 min on ice and then was sonicated on ice. The lysate was centrifuged for 20 min at 160,000 g, and the supernatant was quick-frozen with liquid nitrogen and stored at  $-80^{\circ}\text{C}$ . Lysates were prepared from SN tissues in a similar fashion. Protein concentrations of the lysates were quantified using the method of Bradford (1976). Lysates (50  $\mu\text{g}$  of protein) were incubated at  $37^{\circ}\text{C}$  in a buffer of 25 mM HEPES (pH 7.5), 10% sucrose, 0.1% CHAPS, and 10 mM dithiothreitol with the fluorogenic substrate DEVD-7-amino-4-trifluoromethylcoumarin (15  $\mu\text{M}$ ; Enzyme Systems Products). Cleavage of substrate was monitored over time in an SLM 8000 fluorometer (excitation, 400 nm; emission, 505 nm) as previously described (Stefanis et al., 1996). Each sample was incubated with or without pretreatment for 15 min with 1  $\mu\text{M}$  DEVD-fluoromethyl ketone (Enzyme Systems Products). The cleavage of substrate in the presence of these saturating concentrations of this inhibitor reflects background nonspecific activity. Therefore, caspase-3 DEVD-cleaving activity for each sample was calculated as the difference between the rate of cleavage in the absence and presence of the inhibitor.

## RESULTS

### Caspase-3 expression in normal postnatal SN

A single protected band of the anticipated size was demonstrated by RPA performed on total mRNA derived from microdissected SN tissue from PND 7 (Fig. 1A) and PND 14 (data not shown) animals, indicating that caspase-3 mRNA is present. We confirmed by western blot that a translation product, the 32-kDa zymogen form of caspase-3, is also present in these tissues (Fig. 1B). In addition to a major band at the expected molecular mass of 32 kDa, we also identified two minor bands at higher molecular mass: one at  $\sim 35$  kDa and a second at  $\sim 50$  kDa (Fig. 1B). Other reports have demonstrated minor bands at higher molecular masses in adult rat (Chen et al., 1998; Namura et al., 1998) and in human kidney and liver (Krajewska et al., 1997). In the immature SN, the band at 35 kDa appears especially prominent in comparison with adult rat cortex (Chen et al., 1998). Whether this pattern of expression is unique to the SN or to the developmental interval we have studied remains to be determined. We have previously shown that natural cell death occurs in the SN (Janec and Burke, 1993; Oo and Burke, 1997). To determine whether the zymogen form of caspase-3 is processed to the activated form in the context of natural cell death in the SN, we performed immunohistochemistry for the p17 subunit. This procedure demonstrated the presence of p17 immunoreactivity exclusively within profiles that also contained apoptotic chromatin clumps (Fig. 1C).

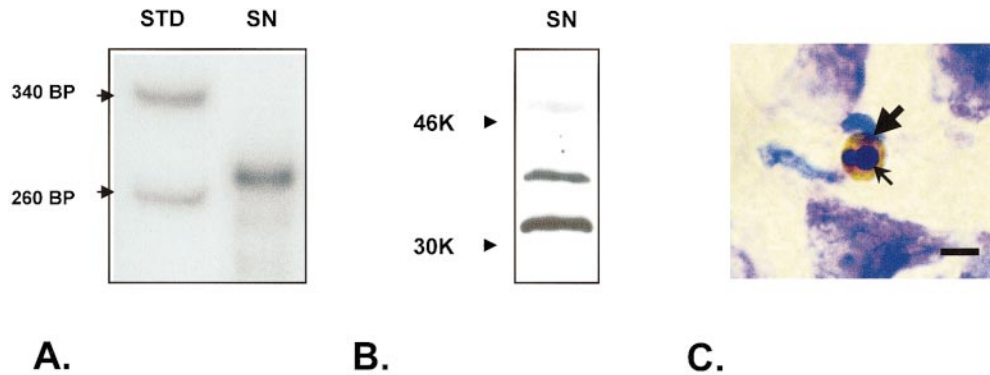


**FIG. 1.** Expression of caspase-3 in normal postnatal rat SN. **A:** RPA for caspase-3 mRNA. A protected band for caspase-3 mRNA is demonstrated for a total RNA preparation derived from SN at PND 7. Molecular weight standards (STD) were generated by end-labeling of pUC19 *Sau3A* restriction digest fragments. The double-stranded RNA hybrid electrophoreses at a slightly slower rate on the gel in comparison with double-stranded DNA of comparable size (Sambrook et al., 1989). **B:** Western blot demonstrates the zymogen form of caspase-3 in SN at PND 7. SN homogenate was probed with an anti-human caspase-3 polyclonal antibody (Upstate Biotechnology), and a major band was demonstrated at 32 kDa. Two additional minor bands were demonstrated at higher molecular masses as discussed in Results. **C:** Immunoperoxidase staining of the p17 subunit of caspase-3 in normal SN at PND 13. Brown peroxidase reaction product (large solid black arrow) is observed surrounding two basophilic apoptotic chromatin clumps identified by thionin counterstain (one clump is identified by a small solid arrow). In normal SN, p17 peroxidase staining was observed strictly within profiles containing apoptotic chromatin clumps. Bar = 5  $\mu$ m.

#### Activation of caspase-3 in SN in PCD induced by striatal lesion

Following excitotoxic injury to the striatum, there was an induction of the number of apoptotic profiles in the SN, identified by thionin stain of chromatin clumps, by 24 h postlesion, as previously reported (Macaya et al., 1994; Kelly and Burke, 1996) (Fig. 2A). At 24 h, when apoptotic death was induced on the experimental (striatal lesion) side, an increase in the number of p17 immunoperoxidase stain-positive profiles was also observed (Fig. 2B). Among six animals studied at 24 h postlesion, 922 p17-positive profiles were examined in the experimental SN; all of them contained apoptotic chromatin clumps (Fig. 3). Conversely, of apoptotic profiles in the experimental SN, 59% were p17-positive. In the SN, immunoreactivity was always observed in the form of circular profiles  $\sim 5 \mu$ m in diameter, surrounding apoptotic chromatin clumps. Such profiles resembled nuclei. In the adjacent mamillary body, where we also observe induced death in this model, p17 immunoreactivity was also always colocalized with apoptotic chromatin clumps (Fig. 3). In both mamillary body and SN, p17 immunoreactivity was occasionally observed within the nucleus of an intact neuron, identified by abundant cytoplasm, a polygonal appearance, and neural processes on Nissl stain (Fig. 3A). We never observed p17 positivity in the cell cytoplasm or in neural processes in this model.

In the striatal injury model, at both PND 7 and 14, we have observed no difference in the number of apoptotic profiles between the contralateral side of animals with unilateral striatal lesions and either the ipsi- or contralateral side of vehicle-injected animals (Macaya et al., 1994; Kelly and Burke, 1996). Therefore, apoptotic profiles on the contralateral side represent ongoing natural cell death in SN (Janec and Burke, 1993; Oo and Burke, 1997), certainly at 4 h postlesion, before induction of cell

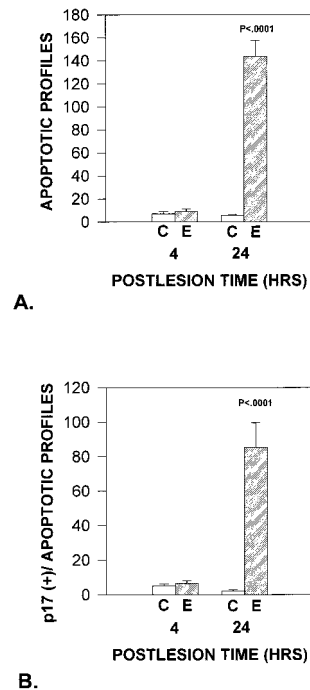


**FIG. 2.** Number of apoptotic profiles and p17-positive profiles in SN following striatal lesion at PND 12. **A:** The number of apoptotic profiles defined by thionin stain of nuclear chromatin clumps markedly increases in SN on the side of striatal injury at 24 h postlesion ( $p < 0.0001$  by one-way ANOVA and Student–Newman–Keuls post hoc analysis). At 4 h, the number of profiles is small and about equal on the experimental (E) and control (C) sides. These profiles are likely to reflect ongoing natural cell death at this developmental age (Janec and Burke, 1993). **B:** The number of p17-positive profiles also increases markedly at 24 h postlesion ( $p < 0.0001$ ). All of these profiles contained intranuclear chromatin clumps, typical of apoptosis, as shown in Fig. 3.

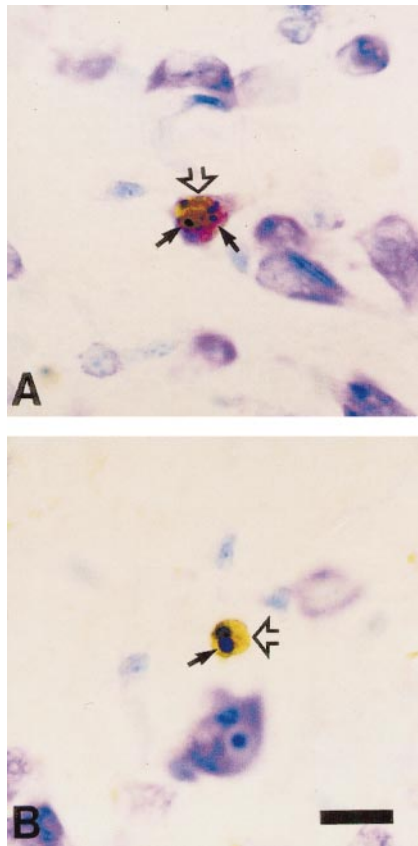


**FIG. 3.** Immunostaining for the p17 subunit of activated caspase-3 following striatal target injury. **A:** A p17-positive apoptotic profile (open arrow) in the adjacent mamillary body at 24 h after striatal lesion. This profile is a neuron with a p17-positive nucleus containing multiple distinct, rounded chromatin clumps (small solid arrows) indicative of apoptosis. **B:** A p17-positive apoptotic profile (open arrow) in the SNpc at 24 h after striatal lesion is indicated by brown chromogen deposition. This profile is 5  $\mu$ m in diameter, and it encompasses two distinct, rounded, basophilic chromatin clumps (one is marked by a small solid arrow), typical of apoptosis. This morphologic appearance is identical to what was observed in the few profiles observed on the contralateral noninjected control side and in normal animals at this postnatal age (Fig. 1C). Bar = 10  $\mu$ m.

death. Positivity for p17 was observed in apoptotic profiles in SN at 4 h, and it displayed cellular features identical to those observed in the setting of both natural cell death (Fig. 1C) and induced death; it was located either in the nucleus of neurons with apoptotic chromatin clumps or in a small circular profile surrounding chromatin clumps. As for induced death, not all apoptotic profiles in the control SN were positive for p17 immunoreactivity; ~60% were.

In spite of the increase in the number of p17-positive profiles in the SN with induced cell death, there was no change (either an increase or decrease) in the abundance of the zymogen form (Fig. 4A) and no increase in content of the p17 subunit, based on western analysis in 12 animals (Fig. 4B). Nevertheless, there was an increase in the level of caspase-3-like activity in the experimental

SN tissues at 24 h postlesion (Fig. 5), corresponding to the time of an increased number of p17-positive apoptotic profiles. Thus, the increase in p17 immunoreactivity was associated with an increase in functional enzyme activity.

**Caspase-3 mRNA expression in PCD induced by striatal lesion**

To determine whether the increased abundance of p17-positive profiles may be mediated, at least in part, by increased transcription of mRNA for the zymogen form of the protein, we assayed caspase-3 mRNA by RPA at both 4 and 24 h postlesion in PND 7 animals. Measurements in nine animals at both time points did not demonstrate an increase in mRNA expression (Table 1 and Fig. 6A). Northern analysis likewise failed to demonstrate a change in mRNA content (Fig. 6B). We considered the possibility that RPA and northern analysis, performed on tissue homogenates, may have lacked the sensitivity to detect small, regional changes. We therefore performed *in situ* hybridization on SN sections in two and three animals at 4 and 24 h, respectively. However, this analysis also did not demonstrate an induction of caspase-3 mRNA on the side of induced death (data not shown). We therefore conclude that the increase in caspase-3 p17-positive profiles is not due to an increased level of mRNA for the zymogen.

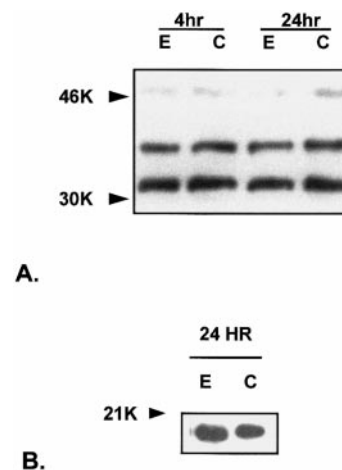


**FIG. 4.** Western blots of SN lysates with antibodies to the caspase-3 zymogen form and the p17 subunit of the activated form. **A:** A representative western blot of lysates prepared from single experimental (E) and control (C) animals at 4 and 24 h after striatal lesion. Fifty micrograms of protein was loaded in each lane, and the blot was probed with anti-human caspase-3 (Upstate Biotechnology). There was no apparent change in abundance of the 32-kDa zymogen form at the time of induced PCD at 24 h postlesion. Each time point was examined in four animals with comparable results. **B:** A representative western blot of lysates prepared from single animals at 24 h after striatal lesion, the time of an increased number of p17-positive profiles (see Fig. 2). There was no consistent visible difference in the intensity of the band demonstrated at 17 kDa between the E and C sides. Twelve animals were examined.

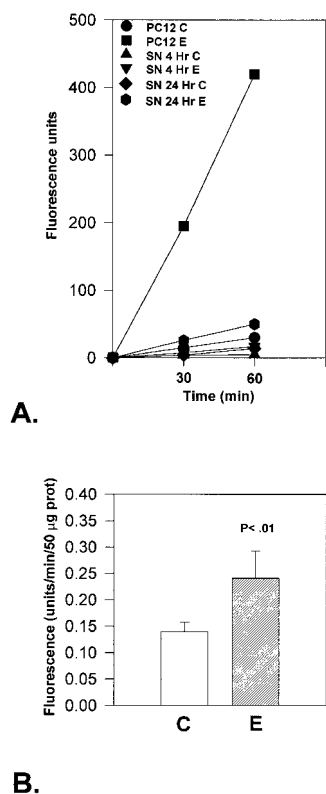


**FIG. 5.** Caspase-3-like activity determined by fluorometric assay. **A:** Caspase-3 activity was measured in SN in single representative animals at 4 h and 24 h postlesion on the side of striatal lesion [experimental (E)] and the contralateral control (C) side in comparison with PC12 cultures at 3 h after serum deprivation to induce apoptosis as a positive control. Caspase-3 activity in the tissue samples was measurable but only a fraction of that in the PC12 cultures. **B:** Caspase-3 activity in paired E and C SN samples ( $n = 15$ ) at 24 h after striatal lesion. There was a small, but significant, induction of caspase-3 activity in the E SN ( $p < 0.01$ ).

#### Activation of caspase-3 in SN in PCD induced by 6-OHDA lesion

To determine whether activation of caspase-3 is a feature of other models of induced PCD in SN neurons

**TABLE 1.** RPA of caspase-3 mRNA in SN following striatal injury at PND 7

Time postlesion	n	Experimental	Control	<i>t</i> test
4	9	0.28 ± 0.10	0.26 ± 0.10	NS
24	9	1.31 ± 0.16	1.25 ± 0.17	NS

Data are as mean ± SEM values, in pg of mRNA/µg of total RNA. At the postlesion times indicated, animals were killed, the SN was microdissected, and total RNA was extracted, as described in Materials and Methods. For each RPA, known amounts of synthetic caspase-3 mRNA were assayed in parallel with tissue samples. Optical densities of the protected bands for these standards were measured on each autoradiogram. These values were used to derive a standard curve from which pg values of caspase-3 mRNA for the tissue samples were derived (see Fig. 6). There was no induction of caspase-3 mRNA in the experimental SNs.

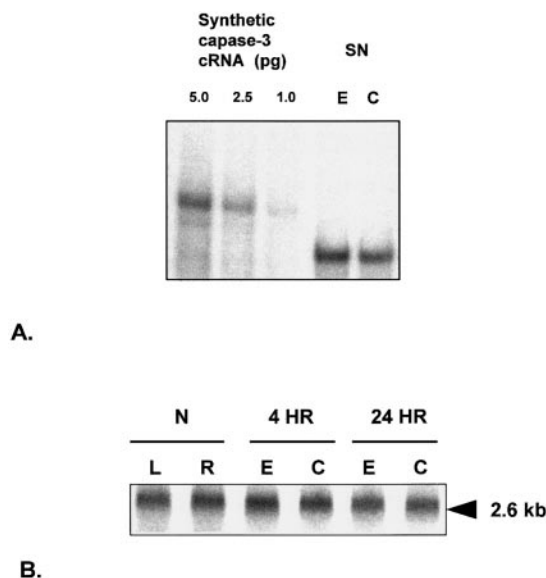


**FIG. 6.** RPA and northern analysis of caspase-3 mRNA in SN following striatal target injury at PND 7. **A:** A representative RPA performed on SN from a single experimental (E) animal at 24 h postlesion. In this assay, standards of synthetic caspase-3 RNA were included, in amounts of 5.0, 2.5, and 1.0 pg per tube. Although in this example there appears to be a more dense protected band on the E side, such a difference was not consistently observed among the nine animals studied (see Table 1). **B:** Northern analysis of caspase-3 mRNA expression in SN in normal (N) animals and in animals at 4 and 24 h after striatal lesion. No difference in mRNA expression was observed on the E side in comparison with the contralateral control (C). L, left; R, right.

and whether it occurs in a model that is more selective for dopamine neurons of the SNpc, we examined its expression following developmental destruction of intrastriatal dopaminergic terminals with 6-OHDA. As previously reported (Marti et al., 1997), this lesion resulted in an induction of apoptotic cell death on day 4 postlesion (Fig. 7A). As in the striatal injury model, this induced death was associated with an increase in the number of p17-positive profiles in SNpc (Fig. 7B). Among four animals studied at 4 days postlesion, 124 apoptotic profiles were identified within the experimental SNpc; 18 (15%) profiles were p17-positive. Most of these profiles showed positive nuclear staining in neurons, colocalized with apoptotic chromatin clumps, as observed in the settings of natural cell death and induced death following striatal lesion. However, in the 6-OHDA model two cellular features were observed in p17-positive profiles that were not observed following striatal injury: Some of the p17-positive nuclei did not contain clearly defined apoptotic chromatin clumps, and in the 6-OHDA model p17 immunoreactivity was not confined to the nucleus. Many of the profiles demonstrated cytoplasmic as well as nuclear staining, and some of these revealed staining of neuronal processes as well as the cell soma (Fig. 8). Thus, p17 immunostaining differs in its intracellular distribution between the striatal injury and

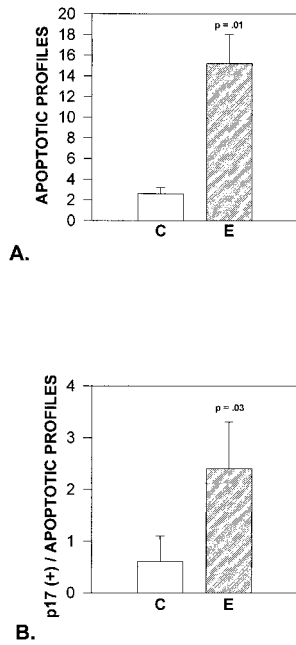


**FIG. 7.** Number of apoptotic profiles and p17-positive profiles in the SNpc from experimental (E) and control (C) animals following intrastriatal injection of 6-OHDA. **A:** The number of apoptotic profiles defined by thionin stain markedly increased in SNpc at 4 days postlesion ( $p = 0.01$ ). **B:** At 4 days postlesion, the number of p17-positive profiles also increased. Note, however, that a smaller percentage of apoptotic profiles is p17-positive (12%) in this model as compared with the striatal injury model.

terminal destruction models of induced death in spite of the fact that identical apoptotic morphology was observed in the two models by conventional techniques, including thionin stain, silver staining, and TUNEL labeling (Marti et al., 1997).

**FIG. 8.** Immunoperoxidase staining of the p17 subunit of activated caspase-3 in SN at 4 days following intrastriatal injection of 6-OHDA. **A:** A representative p17-immunopositive profile in SNpc. The nucleus and cytoplasm of the neuron soma (large solid black arrow) contain brown peroxidase reaction product. In this profile six apoptotic chromatin clumps are demonstrated by thionin counterstain; two are indicated by small black arrows. **B:** A second p17-positive profile in SNpc at 4 days postlesion. Both the nucleus and the cytoplasm of the soma (large solid black arrow) are stained. Reaction product is also observed in an extended neural process (solid black triangles). Two apoptotic chromatin clumps are identified by thionin stain; one is indicated by a small solid arrow. Bar = 10  $\mu$ m.

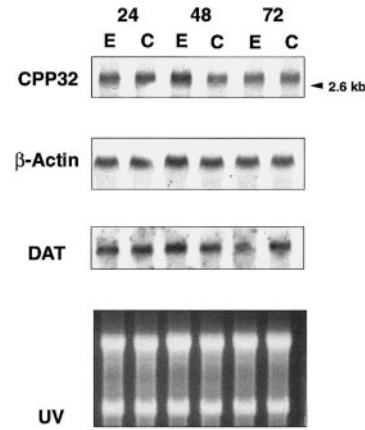
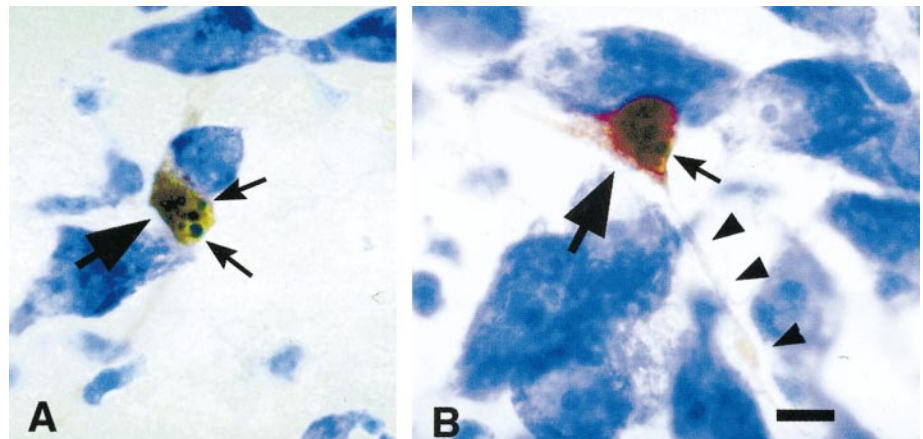


**FIG. 9.** Northern analysis of caspase-3 mRNA expression in SN following 6-OHDA lesion. No consistent difference was noted between the experimental (E) and control (C) sides of the brain at 24, 48, or 72 h after the lesion. The band on the E side at 48 h appears slightly darker, but reprobing of the same blot with a riboprobe for  $\beta$ -actin reveals that there is a slightly higher load of that lane. The blot was stripped again and probed for the dopamine transporter (DAT) to demonstrate that the lesion was effective in reducing expression of a dopamine marker at 72 h postlesion.

In the 6-OHDA model of induced death, we found that, like the target injury model, there was no increase in the expression of caspase-3 mRNA (Fig. 9).

**DISCUSSION**

The principal finding of these investigations is that there is activation of caspase-3 in models of natural and induced PCD in neurons of the SN. Both the striatal injury model and the 6-OHDA terminal destruction model have been shown to induce apoptotic death in

neurons of the SN (Macaya et al., 1994; Marti et al., 1997), resulting in a lasting decrease in the number of neurons. In both models, we identified an increase in the number of profiles immunolabeled with an antiserum specific for the p17 subunit of the active enzyme heterodimer (Armstrong et al., 1997; Namura et al., 1998) at the time of induced apoptotic death. In both models, p17 immunoreactivity correlated not only regionally and temporally with the induction of apoptotic death, but also at a cellular level it strongly correlated with the morphologic appearance of apoptosis. In both models, p17 immunoreactivity, colocalized with apoptotic morphology, could be identified in neurons. In the striatal lesion model, the increase in the number of p17-positive profiles was associated with an increase in caspase-3-like enzyme activity, demonstrated by fluorometric assay. This increase in enzyme activity, in conjunction with the immunohistochemical observations showing an almost universal association between p17 staining and apoptotic morphology, suggests that caspase-3 plays a role in PCD in these models. Nevertheless, it must be recognized that the DEVD-7-amino-4-trifluoromethylcoumarin-cleaving activity could be attributed to a caspase other than caspase-3. In addition, demonstration of the presence of activated caspase-3 does not prove that it is necessary or sufficient for cell death. In paradigms of withdrawal of trophic support from PC12 cells and sympathetic neurons, although caspase-3-like activity was induced, it was found to be neither necessary nor sufficient for cell death (Stefanis et al., 1998).

In all of these settings, whereas p17 immunoreactivity was almost always associated with apoptotic morphology, the converse was not true; many apoptotic profiles were not p17-positive. In the striatal injury model, 59% of apoptotic profiles were p17-positive; in the 6-OHDA model, only 12% were. There are three principal explanations for the appearance of p17-positive and -negative subpopulations of apoptotic profiles. One is that caspase-3 p17 expression occurs early and transiently in the course of cell death, such that it is not always present when apoptotic morphology is apparent. Alternatively, it is possible that there is more than one pathway mediating PCD in these models, and although some of these may use caspase-3, others may not. Third, it may simply be that in tissue sections, not all protein reagents used in immunohistochemistry gain access to all profiles in the section, resulting in some false-negative profiles for p17 immunoreactivity. Each of these explanations may apply. Although false-negative staining is a widely recognized pitfall of immunohistochemistry, it is not likely to explain the far greater percentage of positively stained apoptotic profiles in the striatal injury model as compared with the 6-OHDA model, because sections from these animals were handled in identical fashion. The low percentage of p17-positive profiles in the 6-OHDA model suggests that some apoptotic profiles in that model may not be formed by pathways using caspase-3. This difference between the two models may relate to the different injuries used to induce death, or it may relate to

the fact that the 6-OHDA model is selective for the dopaminergic phenotype, whereas the target injury model is not.

In the striatal injury model of induced PCD, p17-positive profiles were fairly uniform in their appearance. They were either small, circular profiles containing apoptotic chromatin clumps or neurons with p17-positive nuclei and chromatin clumps (see Fig. 3). Because the small circular profiles containing chromatin clumps have the same size and appearance as neuronal nuclei and contain apoptotic chromatin, it is tempting to speculate that they are in fact nuclei and that p17 localization is therefore strictly nuclear in this model. This finding would suggest that in the settings of induced developmental cell death, and natural cell death, in SNpc neurons, caspase-3 is likely to be acting primarily on proteins associated with the nucleus. In addition to poly-(ADP-ribose) polymerase (Kaufmann et al., 1993), proteins postulated to be caspase-3 substrates and that are associated with the nucleus include the sterol regulatory element-binding proteins (Wang et al., 1995), DNA-dependent protein kinase (Song et al., 1996), and the MDM2 oncoprotein (Erhardt et al., 1997).

In the 6-OHDA model, not all p17-positive profiles showed nuclear staining or nucleus-like circular profiles. As shown in Fig. 8, several of these profiles showed cytoplasmic staining, with localization to the cell soma and processes. This distribution, in a model of a pathologic process involving the neurons of the SNpc, is similar to that observed in another model of pathological process, ischemic injury. Namura et al. (1998) have demonstrated, using the same antiserum to p17 that we have used, that following ischemic injury, immunoreactivity is observed in the cytoplasm of cortical neurons. This observation and our own in the 6-OHDA model in comparison with our observations in induced developmental and natural cell death suggest that caspase-3 may have a different cellular localization in different paradigms of PCD in neurons. Its localization to the cytoplasm in the 6-OHDA model has at least two possible interpretations. One is that the caspase-3 proenzyme is activated by proteolytic processing in the cytoplasm in this form of PCD and that it is functionally active in this location, cleaving cytoplasmic proteins. The other possibility is that the active form is primarily localized to the nucleus initially in this form of cell death, but because of disruption of the integrity of the nuclear membrane, it "leaks" into the cytoplasm, where it may or may not continue to function as a caspase. On the basis of our observations at the light microscope level, particularly in neurons like the profile shown in Fig. 8B, we suggest that it is unlikely that such extensive process staining would be observed due strictly to leakage from the nucleus in an otherwise morphologically intact neuron. We would instead speculate that activated caspase-3 is being formed directly in the cytoplasm and is playing a role in the destruction of both the cell soma and the neural processes. In this regard it is important to note that nerve process and terminal degeneration are important early

features of degenerative neurologic disease and that the mechanisms mediating neurite destruction may be quite different from those mediating cell body or nuclear destruction (Deckwerth and Johnson, 1994).

It is notable that based on our prior morphologic assessments of apoptotic death at the light microscope level, using suppressed silver staining, thionin stain for chromatin clumps, and TUNEL labeling, we did not discern a difference in the appearance of apoptotic profiles in the SNpc between the striatal lesion model and the 6-OHDA terminal destruction model. Based on this similarity and given that terminal destruction would abrogate presynaptic terminal-target interactions, we had previously hypothesized that induced apoptotic death in the 6-OHDA model was primarily due to disruption of target-derived support, as in the target lesion model. However, this hypothesis alone cannot account for the differences in p17 immunostaining that we observe between the two models. It is more likely that the cytoplasmic staining is due to a pathologic process, related to an effect of the neurotoxin.

Another interesting feature of p17 immunoreactivity in the 6-OHDA model is that it occasionally (in 16% of instances) was observed in the absence of apoptotic chromatin clumps. This finding suggests that in this model p17 immunoreactivity could serve as an early marker for induced PCD, appearing before morphologic evidence of apoptosis.

In neither the striatal target injury model nor the 6-OHDA model was an increase in the number of p17-positive profiles associated with an increased abundance of mRNA for caspase-3. We therefore conclude that the increase in p17-positive profiles is likely to be related to posttranslational cleavage of the zymogen form. In this respect our results differ from those in an ischemia model, in which increases in mRNA were observed (Chen et al., 1998). However, there is a precedent for posttranslational activation of caspase-3, observed in cultured cerebellar granule cells (Du et al., 1997).

Although immunostaining demonstrated a clear increase in the number of p17-positive profiles in the target injury model, western blotting did not reveal either a decrement in level of the zymogen form or an increase in level of the p17 subunit. The most likely explanation for this apparent discrepancy is that the western analyses, performed on tissue homogenates, lacked both the regional and cellular resolution of the histologic analysis and the quantitative sensitivity. In spite of this discrepancy, it is unlikely that the increase in p17-positive profiles represents an artifact of protein redistribution during cell death, because the increased number of profiles was associated with an increase in caspase-3-like enzyme activity.

This study does not address the nature of the upstream molecular events that lead to activation of caspase-3. We have previously shown, in the striatal target injury model, that induction of cell death correlates regionally and temporally with increased protein expression of c-jun N-terminal kinase (JNK) and c-jun (Oo et al., 1999).

Whether these molecules play an upstream role in the activation of caspase-3 or other caspase family members, as proposed in one model of death in PC12 cells induced by trophic factor withdrawal (Park et al., 1996), remains to be determined.

Given that immunoreactivity for the p17 subunit of activated caspase-3 was observed in natural cell death and two models of induced PCD in neurons of the SNpc, it may be a useful reagent for the investigation of the mechanisms of neuron death in PD and allied disorders that are characterized by loss of SNpc neurons. In relation to PD, although some investigators have identified morphologic evidence of PCD (Mochizuki et al., 1996; Anglade et al., 1997; Tompkins et al., 1997), others have not (Kosel et al., 1997). Undoubtedly, one of the reasons why different investigators have obtained different results is that it is technically very difficult to perform high-quality morphologic studies of human postmortem tissues. The development and application of reagents for molecular components of PCD will broaden the available investigative approaches.

**Acknowledgment:** We are grateful to Ms. Evelyn Alexander for excellent secretarial assistance. This work was supported by grant 26836 from the National Institute of Neurological Disorders and Stroke, the Parkinson's Disease Foundation, the Smart Family Foundation, the Lowenstein Foundation, and a grant from the Lucille P. Markey Trust (to L.S.).

## REFERENCES

- Alnemri E. S. (1997) Mammalian cell death proteases: a family of highly conserved aspartate-specific cysteine proteases. *J. Cell. Biochem.* **64**, 33–42.
- Alnemri E. S., Livingston D. J., Nicholson D. W., Salvesen G., Thornberry N. A., Wong W. W., and Yuan J. (1996) Human ICE/CED-3 protease nomenclature. *Cell* **87**, 171.
- Anglade P., Vyas S., Javoy-Agid F., Herrero M. T., Michel P. P., Marquez J., Mouatt-Prigent A., Ruberg M., Hirsch E. C., and Agid Y. (1997) Apoptosis and autophagy in nigral neurons of patients with Parkinson's disease. *Histol. Histopathol.* **12**, 25–31.
- Armstrong R. C., Aja T. J., Hoang K. D., Gaur S., Bai X., Alnemri E. S., Litwack G., Karanewsky D. S., Fritz L. C., and Tomaselli K. J. (1997) Activation of the CED3/ICE-related protease CPP32 in cerebellar granule neurons undergoing apoptosis but not necrosis. *J. Neurosci.* **17**, 553–562.
- Barde Y. A. (1989) Trophic factors and neuronal survival. *Neuron* **2**, 1525–1534.
- Bradford M. M. (1976) A rapid and sensitive method for the quantitation of microgram quantities of protein utilizing the principle of protein-dye binding. *Anal. Biochem.* **72**, 248–254.
- Bredesen D. E. (1995) Neural apoptosis. *Ann. Neurol.* **38**, 839–851.
- Burke R. E., Franklin S. O., and Inturrisi C. E. (1994) Acute and persistent suppression of preproenkephalin mRNA expression in the striatum following developmental hypoxic-ischemic injury. *J. Neurochem.* **62**, 1878–1886.
- Chen J., Nagayama T., Jin K., Stetler R. A., Zhu R. L., Graham S. H., and Simon R. P. (1998) Induction of caspase-3-like protease may mediate delayed neuronal death in the hippocampus after transient cerebral ischemia. *J. Neurosci.* **18**, 4914–4928.
- Clarke P. G. H. (1985) Neuronal death in the development of the vertebrate nervous system. *Trends Neurosci.* **8**, 345–349.
- Clarke P. G. H. and Oppenheim R. W. (1995) Neuron death in vertebrate development: *in vitro* methods, in *Methods in Cell Biology*, Vol. 46: *Cell Death* (Schwartz L. M. and Osborne B. A., eds), pp. 277–321. Academic Press, San Diego.

- Cowan W. M., Fawcett J. W., O'Leary D. D. M., and Stanfield B. B. (1984) Regressive events in neurogenesis. *Science* **225**, 1258–1265.
- Deckwerth T. L. and Johnson E. M. Jr. (1994) Neurites can remain viable after destruction of the neuronal soma by programmed cell death (apoptosis). *Dev. Biol.* **165**, 63–72.
- Du Y., Bales K. R., Dodel R. C., Hamilton-Byrd E., Horn J. W., Czilli D. L., Simmons L. K., Ni B., and Paul S. M. (1997) Activation of a caspase 3-related cysteine protease is required for glutamate-mediated apoptosis of cultured cerebellar granule neurons. *Proc. Natl. Acad. Sci. USA* **94**, 11657–11662.
- Ellis R. E., Yuan J., and Horvitz H. R. (1991) Mechanisms and functions of cell death. *Annu. Rev. Cell Biol.* **7**, 663–698.
- Enari M., Hug H., and Nagata S. (1995) Involvement of an ICE-like protease in Fas-mediated apoptosis. *Nature* **375**, 78–81.
- Erhardt P., Tomaselli K. J., and Cooper G. M. (1997) Identification of the MDM2 oncoprotein as a substrate for CPP32-like apoptotic proteases. *J. Biol. Chem.* **272**, 15049–15052.
- Fernandes-Alnemri T., Litwack G., and Alnemri E. S. (1994) CPP32, a novel human apoptotic protein with homology to *Caenorhabditis elegans* cell death protein Ced-3 and mammalian interleukin-1 $\beta$ -converting enzyme. *J. Biol. Chem.* **269**, 30761–30764.
- Gavrieli Y., Sherman Y., and Ben-Sasson S. A. (1992) Identification of programmed cell death in situ via specific labeling of nuclear DNA fragmentation. *J. Cell Biol.* **119**, 493–501.
- Gundersen H. J. G. (1986) Stereology of arbitrary particles. *J. Microsc.* **143**, 3–45.
- Hamburger V. (1992) History of the discovery of neuronal death in embryos. *J. Neurobiol.* **23**, 1116–1123.
- Jacobson M. D., Weil M., and Raff M. C. (1997) Programmed cell death in animal development. *Cell* **88**, 347–354.
- Janec E. and Burke R. E. (1993) Naturally occurring cell death during postnatal development of the substantia nigra of the rat. *Mol. Cell. Neurosci.* **4**, 30–35.
- Johnson E. M. and Deckwerth T. L. (1993) Molecular mechanisms of developmental neuronal death. *Annu. Rev. Neurosci.* **16**, 31–46.
- Kaufmann S. H., Desnoyers S., Ottaviano Y., Davidson N. E., and Poirier G. G. (1993) Specific proteolytic cleavage of poly(ADP-ribose) polymerase: an early marker of chemotherapy-induced apoptosis. *Cancer Res.* **53**, 3976–3985.
- Keane R. W., Srinivasan A., Foster L. M., Testa M. P., Ord T., Nonner D., Wang H. G., Reed J. C., Bredesen D. E., and Kayalar C. (1997) Activation of CPP32 during apoptosis of neurons and astrocytes. *J. Neurosci. Res.* **48**, 168–180.
- Kelly W. J. and Burke R. E. (1996) Apoptotic neuron death in rat substantia nigra induced by striatal excitotoxic injury is developmentally dependent. *Neurosci. Lett.* **220**, 85–88.
- Kermer P., Klocker N., Labes M., and Bahr M. (1998) Inhibition of CPP32-like proteases rescues axotomized retinal ganglion cells from secondary cell death in vivo. *J. Neurosci.* **18**, 4656–4662.
- Kerr J. F. R., Wyllie A. H., and Currie A. R. (1972) Apoptosis: a basic biological phenomenon with wide-ranging implications in tissue kinetics. *Br. J. Cancer* **26**, 239–257.
- Kosel S., Egensperger R., von Eitzen U., Mehraein P., and Graeber M. B. (1997) On the question of apoptosis in the parkinsonian substantia nigra. *Acta Neuropathol. (Berl.)* **93**, 105–108.
- Krajewska M., Wang H. G., Krajewski S., Zapata J. M., Shabaik A., Gascoyne R., and Reed J. C. (1997) Immunohistochemical analysis of in vivo patterns of expression of CPP32 (caspase-3), a cell death protease. *Cancer Res.* **57**, 1605–1613.
- Kuida K., Zheng T. S., Na S., Kuan C.-Y., Yang D., Karasuyama H., Rakic P., and Flavell R. A. (1996) Decreased apoptosis in the brain and premature lethality in CPP32-deficient mice. *Nature* **384**, 368–372.
- Macaya A., Munell F., Gubits R. M., and Burke R. E. (1994) Apoptosis in substantia nigra following developmental striatal excitotoxic injury. *Proc. Natl. Acad. Sci. USA* **91**, 8117–8121.
- Marti M. J., James C. J., Oo T. F., Kelly W. J., and Burke R. E. (1997) Early developmental destruction of terminals in the striatal target induces apoptosis in dopamine neurons of the substantia nigra. *J. Neurosci.* **17**, 2030–2039.
- Milligan C. E., Prevette D., Yaginuma H., Homma S., Cardwell C., Fritz L. C., Tomaselli K. J., Oppenheim R. W., and Schwartz L. M. (1995) Peptide inhibitors of the ICE protease family arrest programmed cell death of motoneurons in vivo and in vitro. *Neuron* **15**, 385–393.
- Miura M., Zhu H., Rotello R., Hartwig E. A., and Yuan J. (1993) Induction of apoptosis in fibroblasts by IL-1 beta-converting enzyme, a mammalian homolog of the *C. elegans* cell death gene *ced-3*. *Cell* **75**, 653–660.
- Mochizuki H., Goto K., Mori H., and Mizuno Y. (1996) Histochemical detection of apoptosis in Parkinson's disease. *J. Neurol. Sci.* **137**, 120–123.
- Namura S., Zhu J., Fink K., Endres M., Srinivasan A., Tomaselli K. J., Yuan J. and Moskowitz M. A. (1998) Activation and cleavage of caspase-3 in apoptosis induced by experimental cerebral ischemia. *J. Neurosci.* **18**, 3659–3668.
- Nicholson D. W., Ali A., Thornberry N. A., Vaillancourt J. P., Ding C. K., Gallant M., Gareau Y., Griffin P. R., Labelle M., Lazebnik Y. A., Munday N. A., Raju S. M., Smulson M. E., Yamin T.-T., Yu V. L., and Miller D. K. (1995) Identification and inhibition of the ICE/CED-3 protease necessary for mammalian apoptosis. *Nature* **376**, 37–43.
- Oo T. F. and Burke R. E. (1997) The time course of developmental cell death in phenotypically defined dopaminergic neurons of the substantia nigra. *Dev. Brain Res.* **98**, 191–196.
- Oo T. F., Henchcliffe C., James D., and Burke R. E. (1999) Expression of c-fos, c-jun, and c-jun N-terminal kinase (JNK) in a developmental model of induced apoptotic death in neurons of the substantia nigra. *J. Neurochem.* **72**, 557–564.
- Oppenheim R. W. (1991) Cell death during development of the nervous system. *Annu. Rev. Neurosci.* **14**, 453–501.
- Park D. S., Stefanis L., Yan C. Y. I., Farinelli S. E., and Greene L. A. (1996) Ordering the cell-death pathway—differential-effects of Bc12, an interleukin-1-converting enzyme family protease inhibitor, and other survival agents on jnk activation in serum nerve growth factor-deprived PC12 cells. *J. Biol. Chem.* **271**, 21898–21905.
- Paxinos G. and Watson C. (1982) *The Rat Brain in Stereotaxic Coordinates*. Academic Press, Sydney.
- Sambrook J., Fritsch E. F., and Maniatis T. (1989) *Molecular Cloning, A Laboratory Manual*. Cold Spring Harbor Laboratory Press, Cold Spring Harbor, New York.
- Sauer H. and Oertel W. H. (1994) Progressive degeneration of nigro-striatal dopamine neurons following intrastriatal terminal lesions with 6 hydroxydopamine: a combined retrograde tracing and immunocytochemical study in the rat. *Neuroscience* **59**, 401–415.
- Song Q., Lees-Miller S. P., Kumar S., Zhang Z., Chan D. W., Smith G. C., Jackson S. P., Alnemri E. S., Litwack G., Khanna K. K., and Lavin M. F. (1996) DNA-dependent protein kinase catalytic subunit: a target for an ICE-like protease in apoptosis. *EMBO J.* **15**, 3238–3246.
- Srinivasan A., Roth K. A., Sayers R. O., Shindler K. S., Wong A. M., Fritz L. C., and Tomaselli K. J. (1998) In situ immunodetection of activated caspase-3 in apoptotic neurons in the developing nervous system. *Cell Death Differ.* **5**, 1004–1016.
- Stefanis L., Park D. S., Yan C. Y. I., Farinelli S. E., Troy C. M., Shelanski M. L., and Greene L. A. (1996) Induction of CPP32-like activity in PC12 cells by withdrawal of trophic support. *J. Biol. Chem.* **271**, 30663–30671.
- Stefanis L., Burke R. E., and Greene L. A. (1997) Apoptosis in neurodegenerative disorders. *Curr. Opin. Neurol.* **10**, 299–305.
- Stefanis L., Troy C. M., Qi H., Shelanski M. L., and Greene L. A. (1998) Caspase-2 (Nedd-2) processing and death of trophic factor-deprived PC12 cells and sympathetic neurons occur independently of caspase-3 (CPP32)-like activity. *J. Neurosci.* **18**, 9204–9215.
- Tewari M., Quan L. T., O'Rourke K., Desnoyers S., Zeng Z., Beidler D. R., Poirier G. G., Salvesen G. S., and Dixit V. M. (1995) Yama/ CPP32 $\beta$ , a mammalian homolog of CED-3, is a CrmA-inhibitable protease that cleaves the death substrate poly(ADP-ribose) polymerase. *Cell* **81**, 801–809.
- Thompson C. B. (1995) Apoptosis in the pathogenesis and treatment of disease. *Science* **267**, 1456–1462.

- Tompkins M. M., Basgall E. J., Zamrini E., and Hill W. D. (1997) Apoptotic-like changes in Lewy-body-associated disorders and normal aging in substantia nigral neurons. *Am. J. Pathol.* **150**, 119–131.
- Ungerstedt U. (1971) Histochemical studies on the effect of intracerebral and intraventricular injections of 6-hydroxydopamine on monoamine neurons in the rat brain, in *6-Hydroxydopamine and Catecholamine Neurons* (Malmfors T. and Thoenen H., eds), pp. 101–127. North Holland, Amsterdam.
- Wang X., Pai J. T., Wiedenfeld E. A., Medina J. C., Slaughter C. A., Goldstein J. L., and Brown M. S. (1995) Purification of an interleukin-1 beta converting enzyme-related cysteine protease that cleaves sterol regulatory element-binding proteins between the leucine zipper and transmembrane domains. *J. Biol. Chem.* **270**, 18044–18050.
- Wijsman J. H., Jonker R. R., Keijzer R., van de Velde C. J. H., Cornelisse C. J., and van Dierendonck J.-H. (1993) A new method to detect apoptosis in paraffin sections: in situ end-labeling of fragmented DNA. *J. Histochem. Cytochem.* **41**, 7–13.
- Yakovlev A. G., Knoblach S. M., Fan L., Fox G. B., Goodnight R., and Faden A. I. (1997) Activation of CPP32-like caspases contributes to neuronal apoptosis and neurological dysfunction after traumatic brain injury. *J. Neurosci.* **17**, 7415–7424.
- Yuan J., Shaham S., Ledoux S., Ellis H. M., and Horvitz H. R. (1993) The *C. elegans* cell death gene *ced-3* encodes a protein similar to mammalian interleukin-1 $\beta$ -converting enzyme. *Cell* **75**, 641–652.